



Cite this: *Chem. Commun.*, 2014, 50, 15948

Received 23rd September 2014,
Accepted 29th October 2014

DOI: 10.1039/c4cc07511k

www.rsc.org/chemcomm

The self-assembled structure of toll-like receptor agonist lipopeptides containing the CSK4 peptide sequence is examined in aqueous solution. A remarkable dependence of morphology on the number of attached hexadecyl lipid chains is demonstrated, with spherical micelle structures for mono- and di-lipidated structures observed, but flexible wormlike micelles for the homologue containing three lipid chains. The distinct modes of assembly may have an important influence on the bioactivity of this class of lipopeptide.

Toll-like receptors (TLRs) are involved in the front line of the innate immune response.¹ They are a class of cell surface receptors, found in many organisms. It is now established that TLR2 mediates the cellular response to bacterial lipoproteins.² Immune therapy adjuvants may be targeted to stimulate TLRs.³ Compared to other TLRs, TLR2 appears to mediate a broader range of response to a variety of microbes.⁴ A lipoprotein component of the cell wall of *E. coli* was identified in 1975,⁵ and this led to the development of synthetic TLR2 agonist lipopeptides.

Lipopeptides *N*-acetylated via glycerol-linked cysteines show activity against TLRs in particular TLR2, an observation that has led to the development of commercially available molecules including PAMCSK4, PAM2CSK4, or PAM3CSK4 containing different numbers of hexadecyl (palmitoyl, PAM) chains linked to the glycerol unit linking the peptide CSKKKK (Fig. 1). The dipalmitoyl lipopeptide PAM2CSK4 also shows agonist activity against TLR2.⁶

To our knowledge, the self-assembly of this class of commercially-available lipopeptide has not previously been

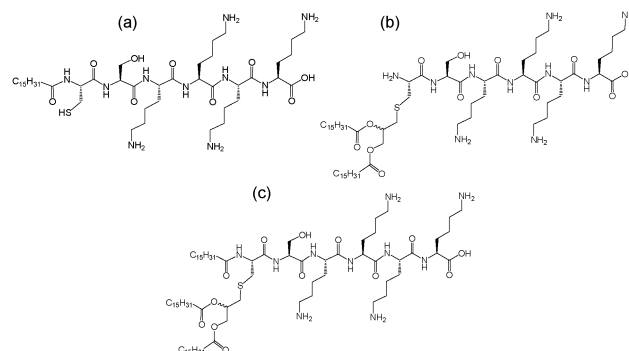


Fig. 1 Molecular structures of (a) PAMCSK4 and (b) PAM2CSK4 and (c) PAM3CSK4.

examined. Here we use the powerful combination of small-angle X-ray scattering (SAXS) and cryogenic-transmission electron microscopy (cryo-TEM) to determine the self-assembled nanostructure for the three lipopeptides PAMCSK4, PAM2CSK4 and PAM3CSK4. In addition, the secondary structure is probed via UV circular dichroism spectroscopy. Remarkable differences in the self-assembly behaviour are observed between the three compounds, in particular PAMCSK4 and PAM2CSK4 form spherical micelles whereas PAM3CSK4 forms wormlike micelles. These unprecedented observations may shed light on the distinct bioactivity of these compounds. Studies show that human TLR types discriminate between different lipopeptide structures including these three compounds.⁴ In particular, PAM3CSK4 preferentially stimulates response to human TLR1 and TLR6, whereas TLR2 and TLR6 respond to PAM2CSK4. A lipopeptide incorporating a cytotoxic T-cell epitope has been shown to self-assemble into fibrils, and this lipopeptide induces an immune response (mouse tumor model) *in vivo*.⁷ This occurred despite the absence of TLR2 activation. PAM2CSK4 and PAM3CSK4 have been used as components within synthetic virus like-particles used in vaccine delivery. Each of the two lipopeptides were linked to a T-helper epitope via a leucine zipper peptide.⁸ The influence of the aggregation

^a Dept of Chemistry, University of Reading, Whiteknights Reading, RG6 6AD, UK.
E-mail: I.W.Hamley@reading.ac.uk

^b National Physical Laboratory, Hampton Road, Teddington, Middlesex, TW11 0LW, UK

^c Department of Applied Physics, Aalto University School of Science, P.O. Box 15100, FI-00076 Aalto, Finland

† Electronic supplementary information (ESI) available: Experimental methods, table of SAXS fitting parameters additional cryo-TEM and SAXS data. See DOI: 10.1039/c4cc07511k

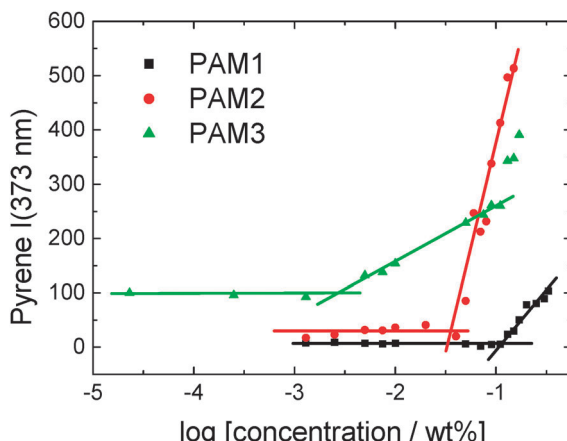


Fig. 2 Concentration dependence of pyrene fluorescence at 373 nm (I_1) for the three lipopeptides. The intersections of the lines shown define the critical aggregation concentrations (cac).

state of the CSK4-based lipopeptides on bioactivity has yet to be elucidated, mainly because the aggregation state has not been investigated to our knowledge. This is the focus of the present study.

We first determined the critical aggregation concentration (cac) for the three lipopeptides using the pyrene fluorescence technique, widely used for other amphiphilic molecules⁹ and more recently for lipopeptides.¹⁰ The concentration-dependent intensity of the I_1 vibronic band of the pyrene fluorescence at 373 nm is shown in Fig. 2. The cacs are determined by the number of lipid chains, having the following values: PAM3CSK4 (cac = 0.003 wt%), PAM2CSK4 (cac = 0.035 wt%) and PAMCSK4 (cac = 0.12 wt%).

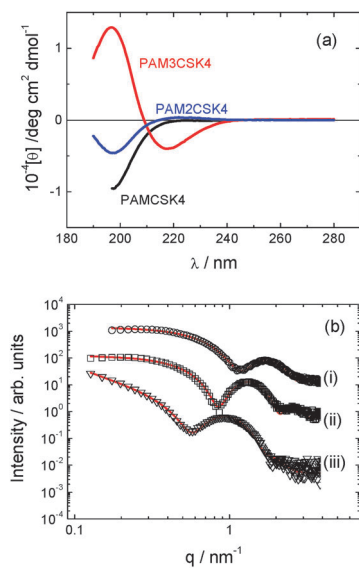


Fig. 3 (a) CD data. (b) SAXS data with form factor models described in text for (a) PAMCSK4, (b) PAM2CSK4, (c) PAM3CSK4. The open symbols are the experimental data, the solid red lines are the model form factor fits described in the text (parameters in Table S1, ESI†). Curves are offset for convenience, and only every 5th data point is shown.

The secondary structure of the peptides within our CSK4 lipopeptide solutions was examined by CD spectroscopy (Fig. 3a). All spectra, and other characterization data presented in this paper, were measured for solutions of the three lipopeptides at 0.5 wt% in LAL (limulus amebocyte lysate) water, as used in bacterial endotoxin assays.

The CD spectra for PAMCSK4 and PAM2CSK4 show a minimum below 200 nm consistent with a disordered conformation. In complete contrast, the spectrum for PAM3CSK4 shows clear features associated with β -sheet secondary structure,¹¹ i.e. a positive maximum near 200 nm and a negative minimum at 217 nm.

The self-assembly of the three lipopeptides was examined using a combination of electron microscopy and small-angle X-ray scattering (SAXS) techniques. Cryo-TEM reveals the presence of spherical micelles in the solutions of PAMCSK4 and PAM2CSK4 (Fig. 4). These have a diameter of approximately 5 nm. Unexpectedly, and in complete contrast, PAM3CSK4 forms worm-like micelles coexisting with globular micelles (Fig. 4c). The wormlike micelles are notably flexible and have a well defined width, in contrast to the highly extended nanotapes/nanobelts observed for other lipopeptides,^{10d,f,g,12} which are also polydisperse in width as a result of a two-dimensional self-assembly process.

SAXS provides support to the findings from cryo-TEM regarding self-assembled nanostructure, and it enables more detail to be obtained on the average dimensions and internal structure of the micellar assemblies. As shown in Fig. 3b, the SAXS profiles measured for the three lipopeptides in dilute solution can be fitted to model form factors for spherical micelles in the case of PAMCSK4 and PAM2CSK4 and for a bilayer structure in the case of PAM3CSK4. The corresponding parameters are listed in Table S1 (ESI†). The external radii of the spherical micelles of PAMCSK4 and PAM2CSK4 are consistent with TEM. A bilayer thickness of 5.3 nm is obtained from the SAXS form factor fit for PAM3CSK4. The molecular length,

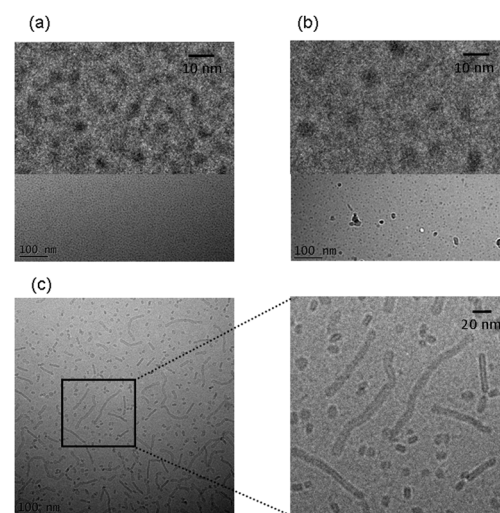


Fig. 4 Cryo-TEM images. (a) PAMCSK, (b) PAM2CSK4, (c) PAM3CSK4. Enlarged images are shown at top in (a, b) and to the right in (c).

considering the length of a hexadecyl lipid chain (*ca.* 1.6 nm) together with the β -sheet forming hexapeptide headgroup (6×0.33 nm (ref. 13) = 2 nm) is estimated to be around 3.6 nm. Therefore the observed 5.3 nm thickness indicates interdigitation of the lipid chains, as observed for other lipopeptides.^{10d,f,g}

As PAM3CSK4 is typically provided commercially as the hydrochloride whereas PAMCSK4 and PAM2CSK4 are provided as TFA salts, we also checked whether the nature of the salt has any effect on PAM3CSK4 self-assembly. No significant influence was revealed by cryo-TEM or SAXS. Fig. S1 (ESI[†]) shows a cryo-TEM image for custom-synthesized PAM3CSK4(TFA) which shows the same morphology of wormlike micelles shown in Fig. 1c. Similarly, the SAXS profiles for PAM3CSK4 TFA and HCl salts are almost identical (Fig. S2, ESI[†]) and the data can be fitted using similar models.

A schematic for the proposed self-assembled structures is shown in Fig. 5. PAMCSK4 and PAM2CSK4 clearly form small spherical micelles, as shown by cryo-TEM and SAXS. The radius of the micelles is consistent with packing of lipopeptides lacking defined secondary structure, consistent with CD. The radius of the micelles determined from SAXS for PAM2CSK4 (3.3 nm) is larger than that for PAMCSK4 (2.2 nm) as expected given the larger volume occupied by the diacyl lipid chains in the former system. All the lipopeptides contain the same peptide with a highly charged tetra-lysine sequence which is sequestered at the surface of the self-assembled nanostructures, this being separated from the lipid core by the CS dipeptide spacer. Distinct from the mono- and di-lipid chain molecules, PAM3CSK4 forms wormlike micelles. In contrast to the extended and rigid nanotapes typically observed for other lipopeptides,^{10d,f,g,12} the self-assemblies of PAM3CSK4, shown by SAXS to contain a bilayer stacking of lipopeptides, resemble more flexible wormlike micelles. Wormlike micelles are not commonly observed for lipopeptides, although they have been reported for a lipopeptide comprising a single palmitoyl chain and the synthetic peptide sequence WAAAAKAAAAKAAAAKA.¹⁴ Based on the cryo-TEM observation of wormlike micelles for PAM3CSK4, combined with SAXS showing a bilayer structure

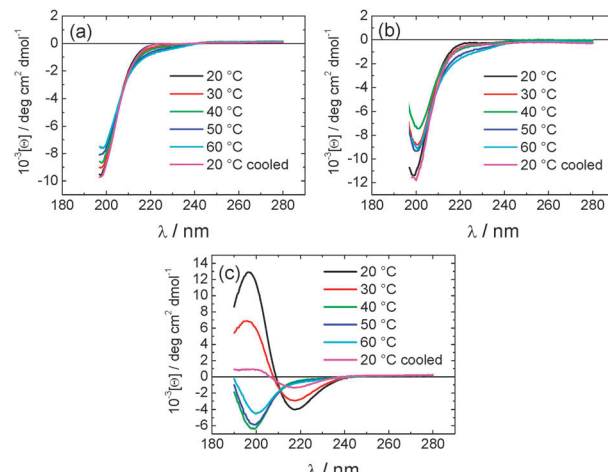


Fig. 6 Temperature dependent CD spectra for (a) PAMCSK4, (b) PAM2CSK4, (c) PAM3CSK4.

and CD which shows β -sheet structure, we propose the self-assembled structure shown in Fig. 5c, *i.e.* flattened wormlike micelles with a bilayer packing of the lipopeptide molecules packed into a β -sheet structure. We presume that the three lipid chains in PAM3CSK4 cannot be accommodated into spherical micelles, and that flattened or ellipsoidal wormlike micelles result from these packing constraints. Our model is consistent with the narrow width distribution for the wormlike micelles notable in the cryo-TEM images, in contrast to the broad distribution of widths observed for typical lipopeptide nanotapes.

To investigate the thermal stability of the secondary structures, and the possible role of lipid chain melting, we performed temperature-dependent CD measurements. The results are shown in Fig. 6. Neither PAMCSK4 nor PAM2CSK4 show any significant change in the disordered conformation in the temperature range 20–60 °C which covers palmitoyl lipid chain melting temperatures, *i.e.* the lipid chain melting transition previously observed for palmitoyl lipopeptides.^{12c} In contrast, PAM3CSK4 exhibits a clear discontinuity in spectra between 30 °C and 40 °C, from a β -sheet conformation at lower temperature to disordered at high temperature. This transition is partially reversible. We associate this transition with the lipid chain melting transition within the tri-palmitoyl chain lipopeptide. The transition from the lipid gel to sol state (at around 40 °C) has previously been shown to change the nanostructure of self-assemblies (twisted ribbons or tapes) of gemini C₁₆ surfactants.¹⁵ In the case of PAM3CSK4 the lipid chain melting may drive a morphological transition. This is currently under further investigation.

Our findings concerning the distinct modes of self-assembly of this class of lipopeptide depending on the number of lipid chains may relate to the bioactivity of these compounds. To our knowledge, the interaction of these lipopeptides with different toll-like receptors has not been correlated to self-assembled nanostructure. Our results should stimulate further efforts to understand whether, and if so by what mechanism, self-assembled

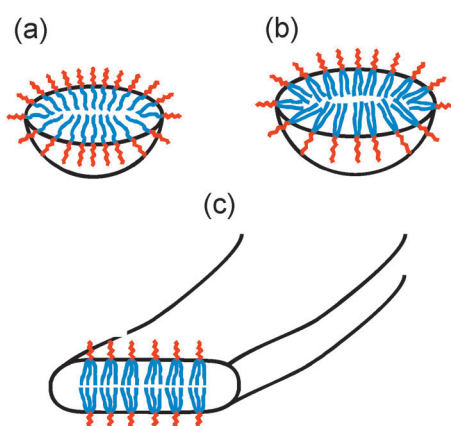


Fig. 5 Model for self-assembled structures of (a) PAMCSK4, (b) PAM2CSK4, (c) PAM3CSK4.



lipopeptide nanostructures interact with toll-like receptors. Also of future interest is the ability to exploit the presence of a cysteine residue in the linker peptide sequence to prepare cross-linked lipopeptide nanostructures.

This work was supported by EPSRC grants EP/G067538/1 and EP/L020599/1 to IWH.

Notes and references

- (a) E. M. Y. Eriksson and D. C. Jackson, *Curr. Protein Pept. Sci.*, 2007, **8**, 412–417; (b) E. J. Mifsud, A. C. L. Tan and D. C. Jackson, *Front. Immunol.*, 2014, **5**, 1–10.
- (a) H. D. Brightbill, D. H. Libratty, S. R. Krutzik, R. B. Yang, J. T. Belisle, J. R. Bleharski, M. Maitland, M. V. Norgard, S. E. Plevy, S. T. Smale, P. J. Brennan, B. R. Bloom, P. J. Godowski and R. L. Modlin, *Science*, 1999, **285**, 732–736; (b) A. O. Aliprantis, R. B. Yang, M. R. Mark, S. Suggett, B. Devaux, J. D. Radolf, G. R. Klimpel, P. Godowski and A. Zychlinsky, *Science*, 1999, **285**, 736–739.
- T. H. Wright, A. E. S. Brooks, A. J. DidSBury, G. M. Williams, P. W. R. Harris, P. R. Dunbar and M. A. Brimble, *Angew. Chem., Int. Ed.*, 2013, **52**, 10616–10619.
- K. O. Omueti, J. M. Beyer, C. M. Johnson, E. A. Lyle and R. I. Tapping, *J. Biol. Chem.*, 2005, **280**, 36616–36625.
- V. Braun, *Biochim. Biophys. Acta*, 1975, **415**, 335–377.
- W. G. Zeng, E. Eriksson, B. Chua, L. Grollo and D. C. Jackson, *Amino Acids*, 2010, **39**, 471–480.
- M. Black, A. Trent, Y. Kostenko, J. S. Lee, C. Olive and M. Tirrell, *Adv. Mater.*, 2012, **24**, 3845–3849.
- A. Ghasparian, T. Riedel, J. Koomullil, K. Moehle, C. Gorba, D. I. Svergun, A. W. Perriman, S. Mann, M. Tamborrini, G. Pluschke and J. A. Robinson, *ChemBioChem*, 2011, **12**, 100–109.
- (a) K. Kalyanasundaram and J. K. Thomas, *J. Am. Chem. Soc.*, 1977, **99**, 2039–2044; (b) F. M. Winnik, *Chem. Rev.*, 1993, **93**, 587–614.
- (a) M. O. Guler, R. C. Claussen and S. I. Stupp, *J. Mater. Chem.*, 2005, **15**, 4507–4512; (b) R. Sabate and J. Estelrich, *J. Phys. Chem. B*, 2005, **109**, 11027–11032; (c) V. Castelletto, G. Cheng, B. W. Greenland and I. W. Hamley, *Langmuir*, 2011, **27**, 2980–2988; (d) V. Castelletto, G. Cheng, C. Stain, C. J. Connon and I. W. Hamley, *Langmuir*, 2012, **28**, 11599–11608; (e) R. R. Jones, V. Castelletto, C. J. Connon and I. W. Hamley, *Mol. Pharm.*, 2013, **10**, 1063–1069; (f) V. Castelletto, R. J. Gouveia, C. J. Connon and I. W. Hamley, *Faraday Discuss.*, 2013, **166**, 381–397; (g) I. W. Hamley, A. Dehsorkhi and V. Castelletto, *Langmuir*, 2013, **29**, 5050–5059; (h) V. Castelletto, R. J. Gouveia, C. J. Connon, I. W. Hamley, J. Seitsonen, A. Nykänen and J. Ruokolainen, *Biomater. Sci.*, 2014, **2**, 362–369; (i) M. Fowler, B. Siddique and J. Duhamel, *Langmuir*, 2013, **29**, 4451–4459.
- (a) C. Toniolo, F. Formaggio and R. W. Woody, in *Electronic Circular Dichroism of Peptides*, ed. N. Berova, P. L. Polavarapu, K. Nakanishi and R. W. Woody, New York, 2012; (b) B. Nordén, A. Rodger and T. R. Dafforn, *Linear Dichroism and Circular Dichroism: A Textbook on Polarized-Light Spectroscopy*, RSC, 2010.
- (a) H. Cui, T. Muraoka, A. G. Cheetham and S. I. Stupp, *Nano Lett.*, 2009, **9**, 945–951; (b) T. J. Moyer, H. Cui and S. I. Stupp, *J. Phys. Chem. B*, 2012, **117**, 4604–4610; (c) V. Castelletto, I. W. Hamley, J. Perez, L. Abezgauz and D. Danino, *Chem. Commun.*, 2010, **46**, 9185–9187; (d) I. W. Hamley, A. Dehsorkhi, P. Jauregi, J. Seitsonen, J. Ruokolainen, F. Coutte, G. Chataigné and P. Jacques, *Soft Matter*, 2013, **9**, 9572–9578; (e) A. Dehsorkhi, V. Castelletto and I. W. Hamley, *J. Pept. Sci.*, 2014, **20**, 453–467; (f) T. Shimada, S. Lee, F. S. Bates, A. Hotta and M. Tirrell, *J. Phys. Chem. B*, 2009, **113**, 13711–13714; (g) J. F. Miravet, B. Escuder, M. D. Segarra-Maset, M. Tena-Solsona, I. W. Hamley, A. Dehsorkhi and V. Castelletto, *Soft Matter*, 2013, **9**, 3558–3564.
- T. E. Creighton, *Proteins. Structures and Molecular Properties*, W. H. Freeman, 1993.
- T. Shimada, N. Sakamoto, R. Motokawa, S. Koizumi and M. Tirrell, *J. Phys. Chem. B*, 2012, **116**, 240–243.
- A. Brizard, C. Aime, T. Labrot, I. Huc, D. Berthier, F. Artzner, B. Desbat and R. Oda, *J. Am. Chem. Soc.*, 2007, **129**, 3754–3762.

